

FAST AND CHEAP SYNTHESIS OF CuO/ZnO THIN FILMS MADE WITH THE SPRAY PYROLYSIS TECHNIQUE

Y. Bellal, A. Bouhank, D. Belfennache*, R. Yekhlief

Research Center in Industrial Technologies CRTI, P.O. Box 64, Cheraga, 16014 Algiers, Algeria

*Correspondence Author e-mail: belfennachedjamel@gmail.com

Received December 26, 2024; revised January 31, 2025; accepted February 7, 2025

In this paper, CuO/ZnO nanocomposites thin films were elaborated with different combination ratio of precursors (copper chloride, zinc chloride) dissolved in distilled water using the spray pyrolysis method in order to study their physicochemical properties. Nanocomposites were elaborated as thin films deposited on the surface of ordinary glass at 550°C using a cheaper and fast technique. Optical, structural and morphological properties of the latter have been examined by UV-vis, X-ray diffraction (XRD), RAMAN, SEM/EDS and AFM. XRD peaks prove the attendance of the polycrystalline models of CuO and ZnO with preferential orientation. Raman shift spectrum confirms the attendance of CuO and ZnO nanocomposites. SEM/EDS and AFM support that there is same roughness on the surface of the ordinary glass RMS=106 nm, which is suitable for the mechanism of photodegradation. In the visible region, we notice a high absorbance and high optical band gaps ($E_{gap}=4.07$ eV) that is suitable for the photodegradation of undesirable substances.

Keywords: *Spray Pyrolysis; CuO/ZnO; Thin Films; Precursor; RAMAN; Photodegradation*

PACS: 73.50.-h, 73.50.Pz

1. INTRODUCTION

Semiconductors attract considerable attention from fundamental and application points of view, due to their widely exploited properties [1-3]. Considerable efforts have been focused on semiconducting metal oxides (TiO₂, MgO, ZnO, CuO, SiO₂, etc), have been the subject of numerous research works and they have attracted great interest in the academic and industrial circles because they present a remarkable improvement in the properties of materials compared to conventional micro and macrocomposites [4-8]. The development of these materials is linked to their interesting physical properties and their advantages over other materials (available, stable, non-toxic, low cost, etc.) [9,10]. These materials (oxides) are good candidates for applications in different technological sectors, particularly in photovoltaics and optoelectronics [11-13]. Currently, the association of two oxides cites great attention from researchers because of their various practical applications such as photocatalyst, sensor, fabrication of microelectronic circuits, piezoelectric devices, fuel cell and solar cells [14-17].

In this case, we have many contents with higher amounts of oxides based on zinc (ZnO) and copper (CuO) that act on semi-conductors with more advantages for different applications. The composite nanostructures of these semi-conductors have a large interface and allow for multiple functional functions and a voice to new applications. The ZnO is a semi-conductor type with a large cross-band direct current (3.37 eV) and a strong exciton energy environment of 60 MeV at the ambient temperature and electrical properties. It is necessary to pay attention to large applications with potential in luminescence, photocatalysts, electricity, gas caps, solar cells, hydrocarbon storage and information [18]. Copper oxide is a beneficial semiconductor material due to its cheaper price, most availability from raw materials and the most important is their non-toxicity. They are used in transistors, spintronic devices, super capacitors, gas sensing electrochromic devices and photocatalysis. The, with a gap of 1.2eV at low temperature [19]. In the Uv-vis domain, its gap energy is 1.2 to 1.7 eV [19,20] which requires a low energy ($h\nu$) for the electron to move from the valence band to the conduction band, but unfortunately it turns out that this gap energy is a little weak to degrade an organic and inorganic pollutants [21]. For that we opt to improve the optical and energetic properties by adding to this semiconductor another n-type semiconductor (ZnO) [21, 22].

This amalgamation can produce interstitial defects which lead the easily passage of the electrons from the valence band to the conduction band by releasing a higher energy to use the oxidation reduction reactions at the semiconductor / pollutant interface (liquid or gas) [21]. The composite nanostructures of these semi-conductors have a large interface and allow for multiple functional functions and a voice to new applications.

Several methods have been used to synthesize ZnO-CuO composites. Among these methods, we can cite Co-precipitation [23], hydrothermal [24]; sol-gel [25] and the Spray Pyrolysis method [26]. The latter offers many manufacturing advantages comparable to the deposition methods, namely the use of available and less expensive equipment, the ability to operate at atmospheric pressure and at low temperature, easy control of manufacturing parameters, compatibility with large deposition surfaces. In this work we study the fast and cheap synthesis of CuO/ZnO thin films made with the spray pyrolysis technique.

2. EXPERIMENTAL PROCEDURE

In this work, we have used a simple device for deposition, it is a small spray perfume bottle filled with a desired precursor solution (copper chloride (S_1) zinc chloride (S_2)), prepared with distilled water at different concentration of precursors as follows: $C_{Total} = 0.05M$ and $V_{Total} = 10ml$ (Fig. 1). The zinc chloride $ZnCl_2 \cdot 2H_2O$ and copper chloride $CuCl_2 \cdot 2H_2O$ are Sigma-Aldrich products with more than 98% of purity.

In the open air with $T_{room} = 25^\circ C$ and $t = 1$ hour, the solutions were prepared. The precursor solutions have been sprayed onto ordinary glasses heated at $550^\circ C$. Before that; the ordinary glasses are cleaned like the previous protocol [21].

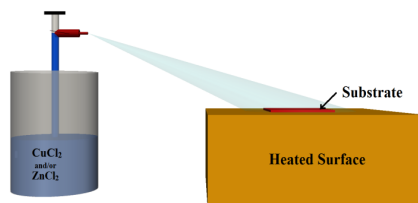


Figure 1. Principle of Spray Pyrolysis

3. RESULTS AND DISCUSSION

3.1 The UV-Visible characterization

ZnO and CuO thin films are n-type and p-type semi-conductors, and the direct result of Zn and Cu gaps in the assembly of the structure leads to the formation of holes in the valence bond. Equations (1) and (2) calculate the gap energy [21].

The optical absorbance spectra of thin films elaborated with different percentage of CuO/ZnO were shown in Figures 2 and 3. The obtained thin films reveal low and strong absorption in the visible region with $a = 381.57nm$ more or less for all thin films. These are the basic characteristics of a solar selective absorber.

In order to determinate the CuO/ZnO band gap energy, the experimental data were extracted and reformed to absorption coefficient (α) as follows [21]:

$$\alpha = \frac{1}{t} \ln \left[\frac{(1-R^2)}{2T} + \sqrt{\frac{(1-R)^4}{4T^2} + R^2} \right] \quad (1)$$

Where

α : Absorption coefficient;

t: Thickness;

R: reflectance;

T: transmittance;

The thickness t is nanometrically scaled Eg and α can be calculated by Tauc eq. (2):

$$\alpha h\nu = A(h\nu - E_g)^n \quad (2)$$

Where h is the photon energy, A is an independent constant of the energy and n is 2 or 0.5 for the indirect and direct allowed transition respectively, for this reason, the gap energy can be computed by extrapolating the linear part of the plot $(\alpha h\nu)^2$ with respect to $h\nu$ (Fig. 3) [21]. we can see that the crystallite sizes of the CuO and ZnO are the responsible factors who can give same band gap variation. In this work, the connection between the band gap and crystallite size was investigated previously [27]. As a result, by adding another precursor the crystallite size is increased. Thus, a high crystallite size is, a band gap is. [27]. CuO is 3.7 eV gap energy in water less than what we found in this work, $E_g = 4.07$ eV for equimolar concentration of precursor solution (50 % $ZnCl_2$; 50% $CuCl_2$). For this reason, we believe that the equi-concentration of the precursor gives the good results for the photodegradation of pollutants.

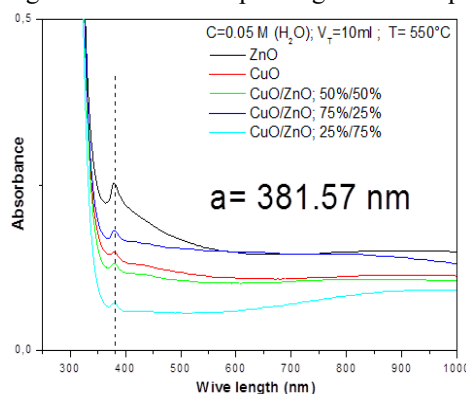


Figure 2. Different optical absorbance of CuO/ZnO nanocomposite thin films

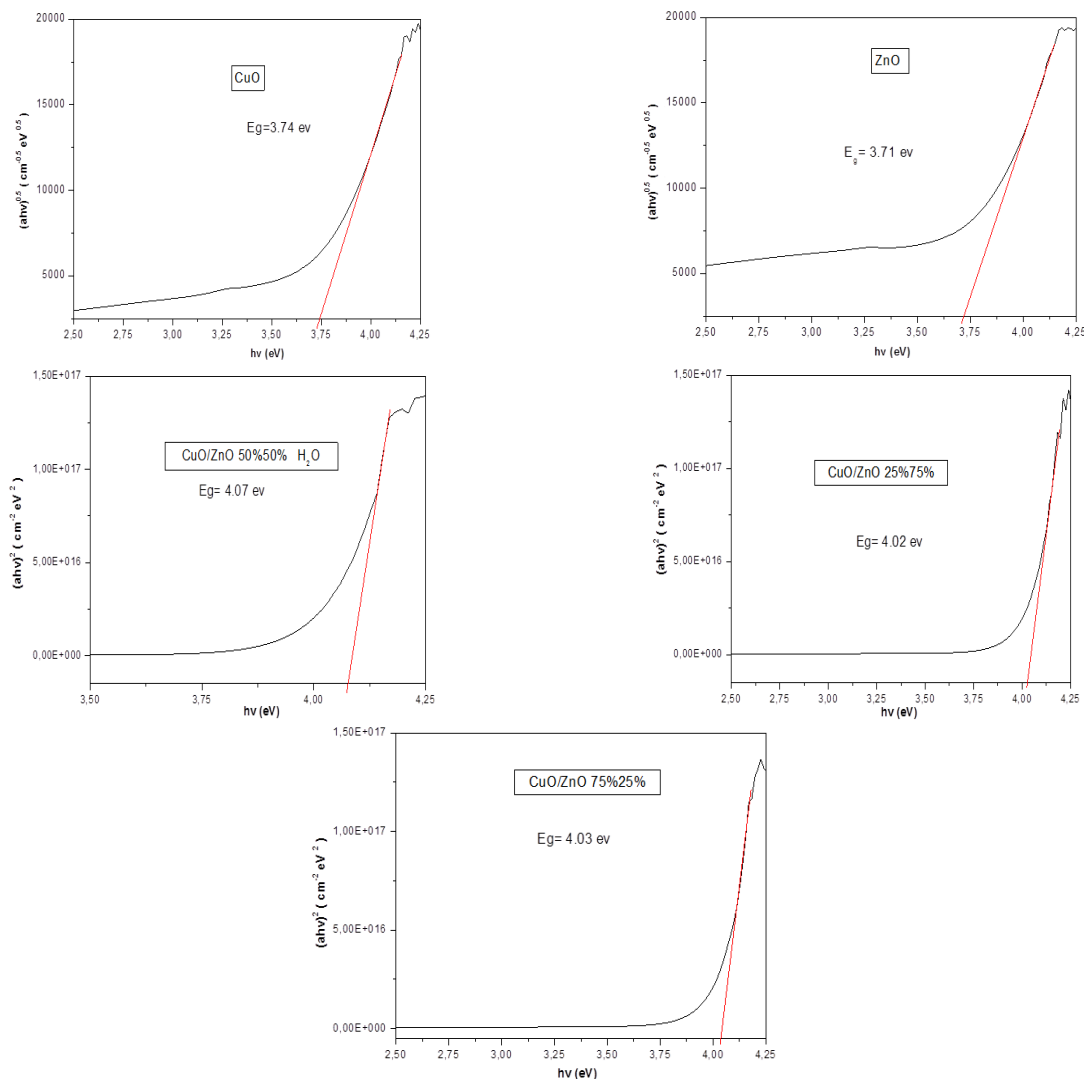


Figure 3. Different Band Gap of CuO/ZnO nanocomposites thin films

3.2. XRD Characterization & Crystallites Sizes Calculation

Fig.4 show the X-ray diffraction spectra for CuO/ZnO nano composite film made with the Spray Pyrolysis Technique. while the precursors were added in equi molar concentration, CuO/ZnO nano composites thin films formed show a various intensity of peaks at 2theta: 16.39, 37.51, 41.32, 43.50, 56.39 and 68° corresponding to the diffraction planes of CuO and ZnO with monoclinic crystalline arrangement. This observation is in good agreement with the JCPDS card 89-5899 for monoclinic crystalline structure

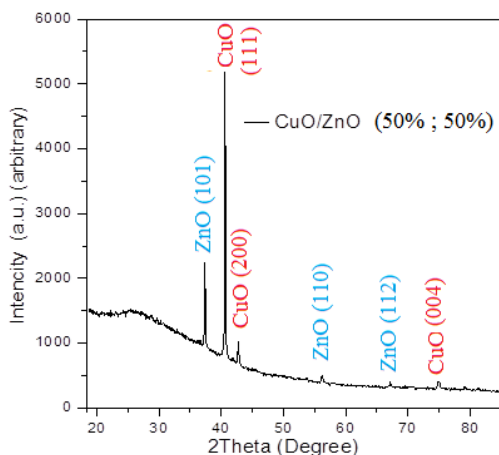


Figure 4. X-ray diffraction of CuO/ZnO thin films at T=550°C

Using Scherrer equation [27, 28]: Crystallite size can be deduced from XRD spectrum from several peaks mentioned below:

$$D = \frac{k\lambda}{W \cos\theta} \quad (3)$$

Where:

D: Crystallites size

K: shape factor named "Scherrer constant" (K=0.9)

W: Full width at half maximum (FWHM) expressed in radians and θ represents the peak position (radians)

λ : Wavelength of X-ray sources ($\text{Cu}_{K\alpha} = 1.5406 \text{ \AA}$).

We notice that CuO/ZnO grain sizes produced at homogeneous mixture of the precursors solution (copper chloride (S_1) zinc chloride (S_2)) are in nanometric scale with a small increase of 15 to 30 nm unlike CuO/ZnO elaborated independently [29-31]. We can gather the crystallites sizes values calculated by (3) in Table 1.

Table 1. Crystallites sizes values

Peaks ($2\theta^\circ$)	Plane (hkl)	Crystallite size (nm)
37.36	101	27.56
40.58	111	41.76
42.73	200	12.01
56.20	110	12.33
67.18	112	26.12
74.90	004	08.97

3.2 Raman Characterization

Raman characterization of CuO-ZnO nanocomposite thin films is an effective method to study the structural and electronic properties of these materials. Raman spectroscopy allows analyzing the vibration modes of chemical bonds in the material, which can provide information on the phase, purity, and interactions between the different phases of the nanocomposite. Figure 5 shows the Raman shift of CuO/ZnO thin films at $T=550^\circ\text{C}$, it shows the presence of the majority of characteristic bands of CuO and ZnO nanocomposite thin films.

In this case, one can expect to observe characteristic peaks related to each phase, as well as interaction or coupling peaks between the two oxides. The main Raman modes for CuO are generally located around 290 cm^{-1} ; 340 and 620 cm^{-1} , while for ZnO the main modes are found around 380 cm^{-1} and 570 cm^{-1} . This is consistent with the results reported in the literatures [21,22].

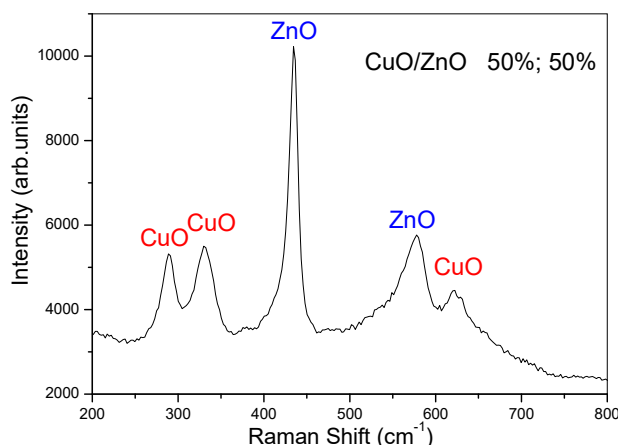


Figure 5. Raman shifts of CuO/ZnO thin films at $T=550^\circ\text{C}$

3.3. Atomic force microscopy (AFM) characterization

In order to better measure the roughness of these samples, we based on the measurement of the factor of roughness RMS to the surface of the software WSxM software [32]. AFM analysis was carried out to observe the surface morphology of CuO/ZnO films. Fig. 6 shows the topographies of the CuO/ZnO thin films at $T=550^\circ\text{C}$, the results of the analysis indicate the presence of islands with different shape, size and number. This is well described according to the "Volmer-Weber" mode i.e. the binding energy between metal ad-atom and substrate atoms is smaller than the binding energy between metal ad-atoms themselves, which leads over potential deposition (OPD) of a 3D metal forming on substrate. For the pulse CuO/ZnO thin films produced with equimolar of precursor shows there is same roughness on the surface of the ordinary glass $\text{RMS}=106 \text{ nm}$, which is suitable for the mechanism of photodegradation in the visible region (Figure 6). By way of comparison, Bünyamin Şahin et al [33] have obtained a roughness lower than found rms values of 60, and 23 nm for ZnO/CuO nanocomposite thin films synthesized by the SILAR (Successive Ionic Layer Adsorption and Reaction) method.

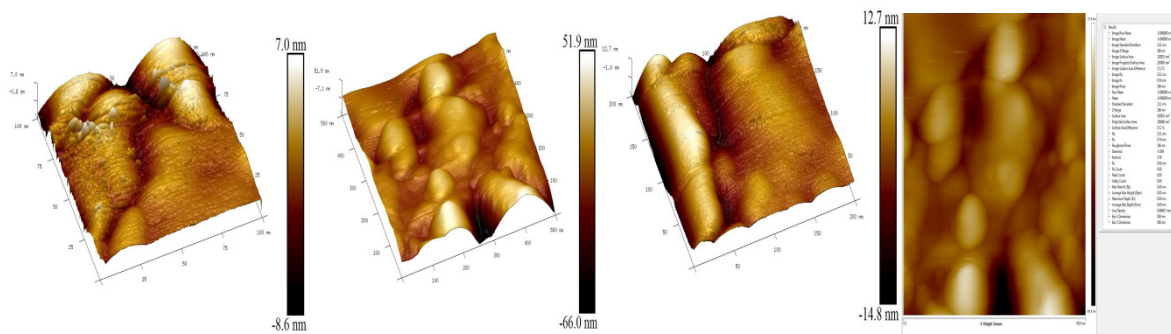


Figure 6. AFM image of CuO/ZnO thin films at T=550°C

3.4 SEM/EDS Characterization

From the Figure 7, we can see that there is a large heterogeneity of deposition on the surface with a nanometrical scale of particle; CuO is spherical form [20] and ZnO is rod with hexagonal form [34] which are suitable for the displacement of the electron from the valance band of CuO to the conductivity band of ZnO that favoure the photodegradation.

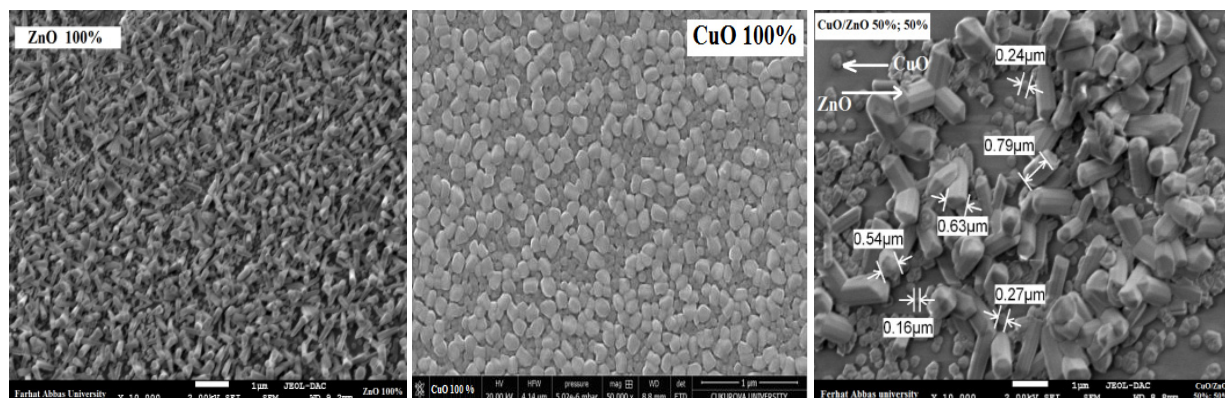


Figure 7. SEM images of CuO/ZnO thin films at T=550°C

In other hand, EDS characterization illustrate that all chemical elements of thin films on the surface of the substrate shows the presence of CuO/ZnO noncomposite arrangement (Fig.8) [21, 22].

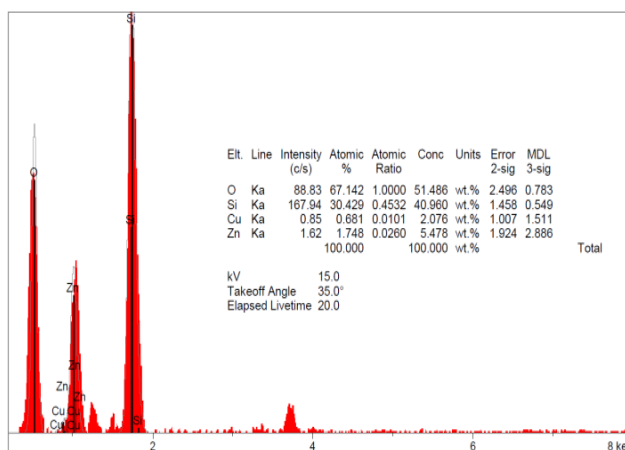


Figure 8. EDS result of CuO/ZnO thin films at T=550°C

4. CONCLUSIONS

This study has made it possible to meet the objectives set concerning the fast and cheap synthesis of CuO/ZnO thin films made with the Spray Pyrolysis Technique. Successful synthesis of thin films samples with the spray pyrolysis technical by different percentage of precursor solution of CuCl₂, 2H₂O and ZnCl₂, 2H₂O, dissolved in distilled water, from the most important results obtained, it is possible to conclude that:

- The UV-Visible characterization shows that all thin films exhibit ultraviolet optical transmission.
- XRD, SEM/EDS and RAMAN characterization of CuO/ZnO nanocomposites confirm the presence of the various phase of CuO and ZnO and the crystallite size are at the nanometrical scale.

Finally, according to these results and compared with the literature CuO and ZnO are suitable for photodegradation of organic and inorganic pollutants. Several issues are still open for future investigation in order to fully understand the synthesis of CuO/ZnO thin films for photodegradation of pollutants. Hopefully, the results presented in this study gives a contribution to this understanding.

Acknowledgements

The authors gratefully acknowledge the support of the Directorate General for Scientific Research and Technological Development of Algeria (DGRSDT). The authors would like to thank Madame Meriem Nechadi from Laboratory of Energy and Solid-State Electrochemistry (L.E.E.S.), Department of Engineering Pro-cess, Faculty of Technology, Ferhat Abbas University Setif-1, Algeria for her help.

ORCID

● Youcef Bellal, <https://orcid.org/0000-0002-8280-9967>; ● Djamel Belfennache, <https://orcid.org/0000-0002-4908-6058>

REFERENCES

- [1] Z. Wang, J. Fan, Y. Zou, X. Fu, L. Shi, Y. Li, X. Ma, *Opt. Commun.* **577**, 131425 (2025). <https://doi.org/10.1016/j.optcom.2024.131425>.
- [2] Y. Benkrima, D. Belfennache, R. Yekhllef, A. M. Ghaleb, *Chalcogenide Lett.* **20**(8), 609-618 (2023). DOI:10.15251/CL.2023.208.609.
- [3] C. Cao, Y. He, Y. Liu, H. Huang, F. Zhang, *Int. J. Prod. Econ.* 109496 (2024) <https://doi.org/10.1016/j.ijpe.2024.109496>.
- [4] R.S. Foumani, E. Fatehifar, and T. Rajae, *Results in Chemistry.* **13**, 101963 (2025), <https://doi.org/10.1016/j.rechem.2024.101963>
- [5] Y. Benkrima, A. Achouri, D. Belfennache, R. Yekhllef, and N. Hocine, *East Eur. J. Phys.* **2**, 215 (2023), <https://doi.org/10.26565/2312-4334-2023-2-23>
- [6] T.G. Gindose, T.B. Atisme, G. Gebreslassie, A.B. Gebresilassie, and E.A. Zereffa, *Materials Advances*, **5**(20), 8017 (2024). <https://doi.org/10.1039/d4ma00357h>
- [7] S. Mahdid, D. Belfennache, D. Madi, M. Samah, R. Yekhllef, and Y. Benkrima, *J. Ovonic. Res.* **19**(5), 535 (2023). <https://doi.org/10.15251/JOR.2023.195.535>
- [8] D. Belfennache, D. Madi, R. Yekhllef, L. Toukal, N. Maouche, M.S. Akhtar, S. Zahra. *Semicond. Phys. Quantum Electron. Optoelectron.* **24**(4), 378-389 (2021). <https://doi.org/10.15407/spqeo24.04.378>
- [9] R. Papitha, V. Hadkar, N.K. Sishu, S. Arunagiri, S.M. Roopan, and C.I. Selvaraj, *Ceramics International*, **50**(20), 39109 (2024). <https://doi.org/10.1016/j.ceramint.2024.07.277>
- [10] S. Zaiou, O. Beldjebli, D. Belfennache, M. Tayeb, F. Zenikheri, and A. Harabi, *Digest J. Nanomater. Biostruct.* **18**(1), 69 (2023). <https://doi.org/10.15251/DJNB.2023.181.69>
- [11] A. Pandey, P. Yadav, A. Fahad, P. Kumar, and M.K. Singh, *Ceramics International*, **50**(12), 21417 (2024). <https://doi.org/10.1016/j.ceramint.2024.03.253>
- [12] Z. Yin, Y. Zeng, D. Yang, Y. Jiao, J. Song, P. Hu, H. Fan, and F. Teng, *Journal of Luminescence*, **257**, 119762 (2023) <https://doi.org/10.1016/j.jlumin.2023.119762>
- [13] R. Ouldamer, D. Madi, and D. Belfennache, in: *Advanced Computational Techniques for Renewable Energy Systems. IC-AIRES 2022*. edited by M. Hatti, *Lecture Notes in Networks and Systems*, **591**, 700 (2023). (Springer, Cham). https://doi.org/10.1007/978-3-031-21216-1_71
- [14] A. Gebretsadik, B. Kefale, C. Sori, D. Tsegaye, H.C.A. Murthy, and B. Abebe, *RSC Advances*. **14**(41), 29763 (2024). <https://doi.org/10.1039/d4ra05989a>
- [15] S-M. Lam, J-C. Sin, W.W. Tong, H. Zeng, H. Li, L. Huang, H. Lin, and J-W. Lim, *Chemosphere*, **344**, 140402 (2023). <https://doi.org/10.1016/j.chemosphere.2023.140402>
- [16] Chitralkha, I. Maurya, S. Shankar, S. Gaurav, V. Tuli, J. Shah, and R.K. Kotnala, *Mater. Chem. Phys.* **291**, 126690 (2022). <https://doi.org/10.1016/j.matchemphys.2022.126690>
- [17] R. Ouldamer, D. Belfennache, D. Madi, R. Yekhllef, S. Zaiou, and M.A. Ali, *J. Ovonic. Res.* **20**(1), 45 (2024). <https://doi.org/10.15251/JOR.2024.201.45>
- [18] C.V. Niveditha, M.J. Fatima, and S. Sindhu, *J. Electrochem. Soc.* **163**, H426 (2016). <https://doi.org/10.1149/2.0971606jes>
- [19] K.E. Brown, and K.S. Choi, *Chem. Commun.* **31**, 3311 (2006). <https://doi.org/10.1039/b604097g>
- [20] Y. Bellal, A. Bouhank, H. Serrar, T. Tüken, and G. Sığircık, *MATEC Web Conf.* **253**, 03002 (2019). <https://doi.org/10.1051/mateconf/201925303002>
- [21] Y. Bellal, and A. Bouhank, *Int. J. Nanosci.* **20**(03), 2150029 (2021). <https://doi.org/10.1142/S0219581X21500290>
- [22] X. Zhao, P. Wang, and B. Li, *Chemical Communications*, **46**(36), 6768 (2010). <https://doi.org/10.1039/c0cc01610a>
- [23] N. Abraham, and S. Aseena, *Materials Today: Proceedings*, **43**, 3698 (2021). <https://doi.org/10.1016/j.matpr.2020.11.406>
- [24] X. Guo, W. Ju, Z. Luo, B. Ruan, K. Wu, and P. Li, *Int. J. Hydrogen Energy*, **98**, 1087 (2025). <https://doi.org/10.1016/j.ijhydene.2024.12.117>
- [25] P. Mahajan, A. Singh, and S. Arya, *J. Alloys Compd.* **814**, 152292 (2020). <https://doi.org/10.1016/j.jallcom.2019.152292>
- [26] M.N. Najah, F.A. Rahmania, I. Cahyanti, M. Hesnaty, S.H. Alias, D. Hartanto, W.P. Utomo, *et al.*, *Afr. J. Chem. Eng.* **51**, 188 (2025). <https://doi.org/10.1016/j.sajce.2024.11.009>
- [27] A. Bouhank, and Y. Bellal, *J. Nano Res.* **69**, 23 (2021). <https://doi.org/10.4028/www.scientific.net/JNanoR.69.23>
- [28] B.D. Cullity, in: *Elements of X-ray Diffraction*, (Addison and Wesley Publishing Company Inc. Reading, USA). pp. 32-106 (1978).
- [29] D. Saravanakumar, H.A. Oualid, Y. Brahmi, A. Ayeshamariam, M. Karunainathy, A.M. Saleem, K. Kaviyarasu, *et al.*, *OpenNano*, **4**, 100025 (2019). <https://doi.org/10.1016/j.onano.2018.11.001>
- [30] M. Alrefae, U.P. Singh, and S.K. Das, *J. Phys.: Conf. Ser.* **1973**(1), 012069 (2021). <https://doi.org/10.1088/1742-6596/1973/1/012069>

- [31] D.M. Jundale, P.B. Joshi, S. Sen, and V.B. Patil, J. Mater. Sci.: Mater. Electron. **23**, 1492 (2012). <https://doi.org/10.1007/s10854-011-0616-2>
- [32] I. Horcas, R. Fernández, J.M. Gomez-Rodriguez, J. Colchero, J. Gómez-Herrero; and A.M. Baro, Rev. Sci. Instrum. **78**(1), 013705 (2007). <https://doi.org/10.1063/1.2432410>
- [33] B. Şahin, and T. Kaya, Mater. Sci. Semicond. Process, **121**, 105428 (2021). <https://doi.org/10.1016/j.mssp.2020.105428>
- [34] N.D. Dien, Adv. Mater. Sci. **4**, 1 (2019). <https://doi.org/10.15761/AMS.1000147>

**ШВИДКИЙ ТА ДЕШЕВИЙ СИНТЕЗ ТОНКИХ ПЛІВОК CuO/ZnO, ВИГОТОВЛЕНИХ
ЗА МЕТОДИКОЮ СПРЕЄВОГО ПІРОЛІЗУ**

Ю. Беллал, А. Буханк, Д. Бельфенаше, Р. Єхлеф

Науково-дослідний центр промислових технологій CRTI, Черага, Алджер, Алжир

У цій статті було розроблено тонкі плівки нанокompозитів CuO/ZnO з різним співвідношенням комбінацій прекурсорів (хлорид міді, хлорид цинку), розчинених у дистильованій воді методом розпилювального піролізу з метою вивчення їх фізико-хімічних властивостей. Нанокompозити були розроблені у вигляді тонких плівок, нанесених на поверхню звичайного скла при 550°C за допомогою дешевої та швидкої техніки. Оптичні, структурні та морфологічні властивості останнього були досліджені методами УФ-виділення, дифракції рентгенівських променів (XRD), раманівського розсіювання, SEM/EDS та AFM. XRD-піки доводять присутність полікристалічних моделей CuO та ZnO з переважною орієнтацією. Спектр комбінаційного зсуву підтверджує присутність нанокompозитів CuO та ZnO. SEM/EDS та AFM підтверджують, що на поверхні звичайного скла є однакова шорсткість RMS=106 нм, яка підходить для механізму фотодеградації. У видимій області ми помічаємо високе поглинання та великі оптичні заборонені зони ($E_{gap} = 4,07$ eV), що підходить для фотодеградації небажаних речовин.

Ключові слова: *спрей-піроліз; CuO/ZnO; тонкі плівки; прекурсор; RAMAN; фотодеградація*